Letter | Editors' Suggestion

Quasi-one-dimensional Coulomb drag between spin-polarized quantum wires

Mingyang Zheng,[1] Rebika Makaju,[1] Rasul Gazizulin,[1,2] Alex Levchenko,[3] Sadhvikas J. Addamane,[4] and Dominique Laroche[1,*]

[1]*Department of Physics, University of Florida, Gainesville, Florida 32611, USA*

[2]*National High Magnetic Field Laboratory High B/T Facility, University of Florida, Gainesville, Florida 32611, USA*

[3]*Department of Physics, University of Wisconsin–Madison, Madison, Wisconsin 53706, USA*

[4]*Center for Integrated Nanotechnologies, Sandia National Laboratories, Albuquerque, New Mexico 87185, USA*

(Received 19 June 2025; revised 23 January 2026; accepted 19 February 2026; published 20 March 2026)

One-dimensional (1D) quantum wires provide a versatile platform for studying strong electron-electron interactions and collective excitations under confinement. Coulomb drag between 1D systems offers a powerful probe of Tomonaga-Luttinger liquid (TLL) physics, with theoretical predictions suggesting a distinct power-law in temperature dependencies between the spin-full and the spin-polarized regimes. However, experimental verification has thus far remained limited. Here, we report measurements of reciprocal and nonreciprocal Coulomb drag between vertically coupled quasi-1D disordered quantum wires in the spin-polarized regime. Clear signatures of spin splitting are observed in both the wires' conductance and in the drag signal. The 1D Coulomb drag signal exhibits different power-law behaviors in the spin-full and spin-polarized regimes and follows the same scaling as predicted for the TLL interaction parameters in ballistic wires. These results are in qualitative agreement with theoretical predictions for backscattering-induced drag in the reciprocal regime of single-subband ballistic quantum wires and show these predictions remain valid in the disordered, nonreciprocal, and multiple-subband regimes.

DOI: 10.1103/5yqq-cw73

Strongly correlated electronic phenomena such as correlated insulators [1], electron crystallization [2], and Bose-Einstein condensation [3] underscore the central role of electron-electron interactions across diverse systems. While two-dimensional (2D) systems have uncovered a range of interaction-driven phases [1,4–7], one-dimensional (1D) quantum wires provide an additional controlled and analytically tractable platform for probing such electronic correlations [8–10]. In one dimension, the restricted phase space for scattering and ineffective screening enhance interaction effects, leading to the breakdown of Fermi liquid theory and the emergence of non-Fermi-liquid behavior [8,11]. Instead of the quasiparticle description in Fermi liquid, the low-energy excitations in 1D systems are propagating collective modes of spin and charge density, described by Tomonaga-Luttinger liquid (TLL) theory [11–13].

Coulomb drag provides a sensitive probe of interaction and correlation between two coupled low-dimensional systems [14] and is an ideal technique to study TLLs. In a typical drag measurement, current in one wire (the drive wire) induces a voltage response in a nearby, electrically isolated wire (the drag wire) [15], as shown in Fig. 1(b). Traditionally, Coulomb drag has been explained by the momentum transfer between charge carriers in the drive and drag wires, which is expected to follow the Onsager relations [15–18], yielding a reciprocal signal in clean wires. Another physical interpretation for the phenomena is current rectification, which interprets Coulomb drag as a rectification of the energy fluctuations in the drive circuit [19–21]. In the current rectification formalism, electric fields, both from the drive current and its fluctuations, induce momentum transfer in the drag wire charge carriers. While the current-inducing electrical field generates momentum transfer in the direction of the current flow, its fluctuations induce momentum transfer in random directions. In clean and noncorrelated ballistic systems, the net fluctuating signal remains 0, the Onsager relations are satisfied, and both momentum transfer and current fluctuation yield identical reciprocal drag results within the linear response regime. However, in a nonballistic wire, disorder can generate both symmetric and antisymmetric potential, while the former only breaks the translation symmetry, the latter breaks inversion symmetry and leads to unequal transmission probability for left- and right-moving electrons, and is a necessary condition for rectification effects. Therefore, rectification of both the current-inducing electric field and its fluctuations can result in a nonreciprocal drag signal whose polarity is determined by the microscopic details of the defects' potential in the mesoscopic wires. This rectification or ratchet effect has been observed in Coulomb drag between coupled quantum dots, topological edge states, and mesoscopic quantum wires [22–25]. In these cases, both theoretical approaches produce different predictions [20,26–30] and, to the best of our knowledge, no attempts to explicitly combine strong electron-electron interactions with mesoscopic fluctuations have been reported in the literature.

Experimental studies have confirmed several hallmark signatures of TLL physics in 1D systems, including spin-charge

*Contact author: dlaroc10@ufl.edu

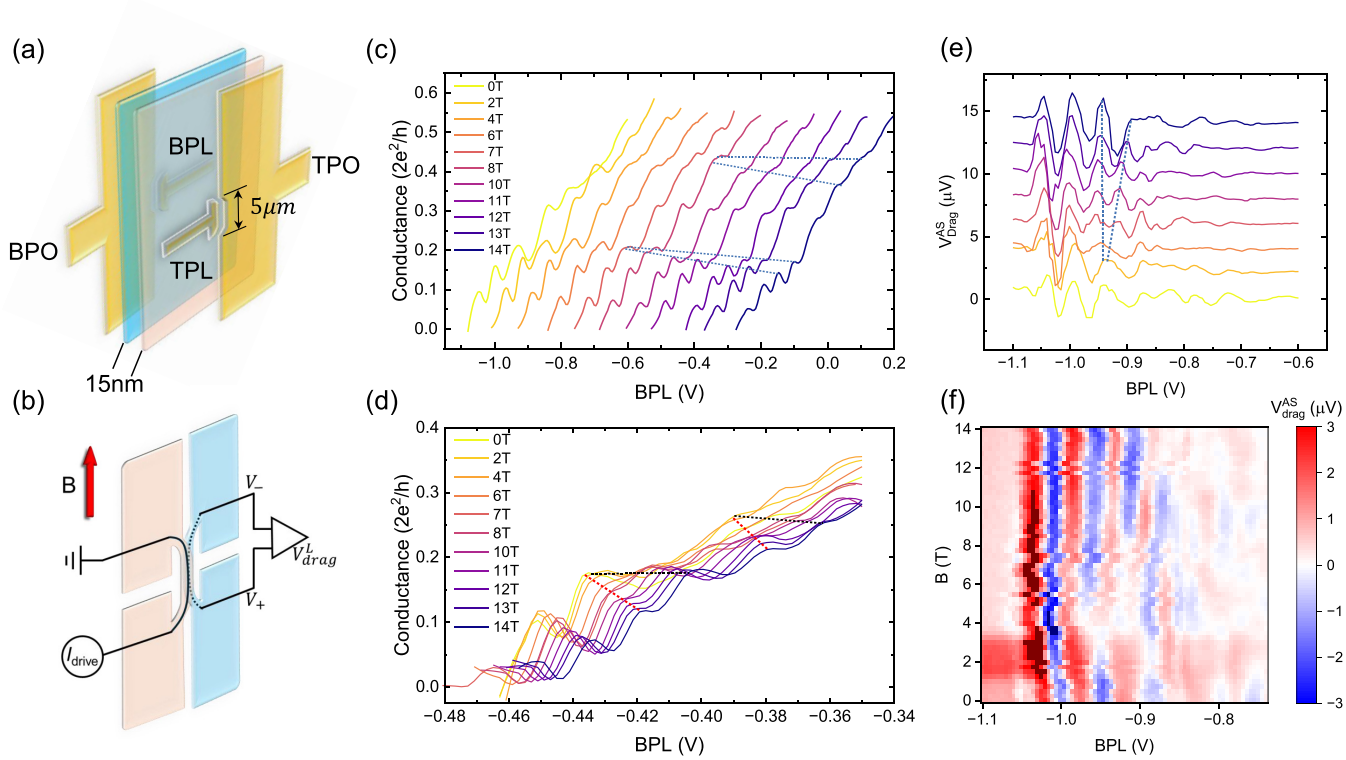

FIG. 1. (a) Schematic of the active part of the double quantum wire device. Each wire consists of a plunger and a pinch-off (PO) gate. (b) In the interacting region of the device, two vertically superimposed independent quantum wires are created, leveraging selective layer depletion with the PO gates. The top (pink) and bottom (blue) layers are depleted to form the drive and drag wires, respectively. The magnetic field is parallel to both wires, with the direction pointing up as shown in the figure. (c) Drag wire conductance as a function of BPL gate voltage at magnetic fields ranging from 0 to 14 T when TPL $= -0.402$ V in scan window 1. Successive lines are horizontally offset by 0.08 V for visibility. The 1D subband plateau features and their spin splitting are clearly seen as the magnetic field increases. The dotted lines are guides to the eye of the spin splittings of the first and second subbands. (d) Drag wire conductance as a function of BPL gate voltage at magnetic fields ranging from 0 to 14 T when TPL $= -1.095$ V in scan window 2. The red dotted lines and black dashed lines are guides for the spin-up and spin-down splitting, respectively. (e) Antisymmetric component of the drag voltage as a function of BPL gate voltage at magnetic fields ranging from 0 to 14 T from bottom to top, when TPL $= -0.402$ V. Successive lines are vertically offset by 2 μV for visibility. The spin-splitting peaks are seen for the first subband around BPL $= -0.94$ V. The left two peaks around BPL $= -1.04$ V and BPL $= -0.99$ V are attributed to defects. (f) Detailed 2D plot of the antisymmetric component of the drag signal as a function of BPL gate voltage and magnetic field for a line cut taken at TPL $= -0.402$ V.

separation, power-law scaling, and the upturn of Coulomb drag resistance at low temperatures [31–35]. While theoretical work has predicted distinctive behavior in Coulomb drag between spin-polarized wires [26], experimental exploration of this regime remains largely uncharted. Given the enhanced role of interactions in spin-polarized 1D systems, investigating Coulomb drag in this regime offers a promising avenue to uncover new many-body phenomena. In this Letter, we report measurements of quasi-1D Coulomb drag between spin-polarized quantum wires. The system consists of two vertically superimposed quantum wires defined electrostatically on a bilayer GaAs/AlGaAs quantum well heterostructure, separated by a thin 15-nm AlGaAs barrier. Each wire is formed within individual two-dimensional electron gases (2DEGs) using surface gates, allowing independent control of their carrier densities and enabling the study of TLL interactions in the multi-subband regime of mesoscopic quasi-1D wires. A magnetic field is applied parallel to the wires to achieve spin polarization without introducing orbital effects. By measuring the density and temperature dependence of the drag response, we probe the interaction mechanisms in both the spin-full and the spin-polarized regimes. This work presents the first experimental investigation of quasi-1D Coulomb drag in the spin-polarized limit and establishes a platform for studying spin-polarized electron-electron interactions.

A schematic of the device is shown in Figs. 1(a) and 1(b), and additional details on device fabrication, measurement techniques, and early device characterization are presented in the Supplemental Material, Secs. 1 and 2 [36] (including Refs. [37–40]). The wire conductance is also shown in the Supplemental Material [36], and both the top and bottom wires exhibit clear 1D conductance plateaus at noninteger values of $2e^2/h$, indicative of subband formation in the nonballistic regime. Owing to its stable subband positions, the top wire is used as the drive wire in the following measurements. By tuning the bottom plunger (BPL) and the top plunger (TPL) gates, the drag signal is measured across various subband configurations in two scan windows defined in Fig. S4 of the Supplemental Material [36].

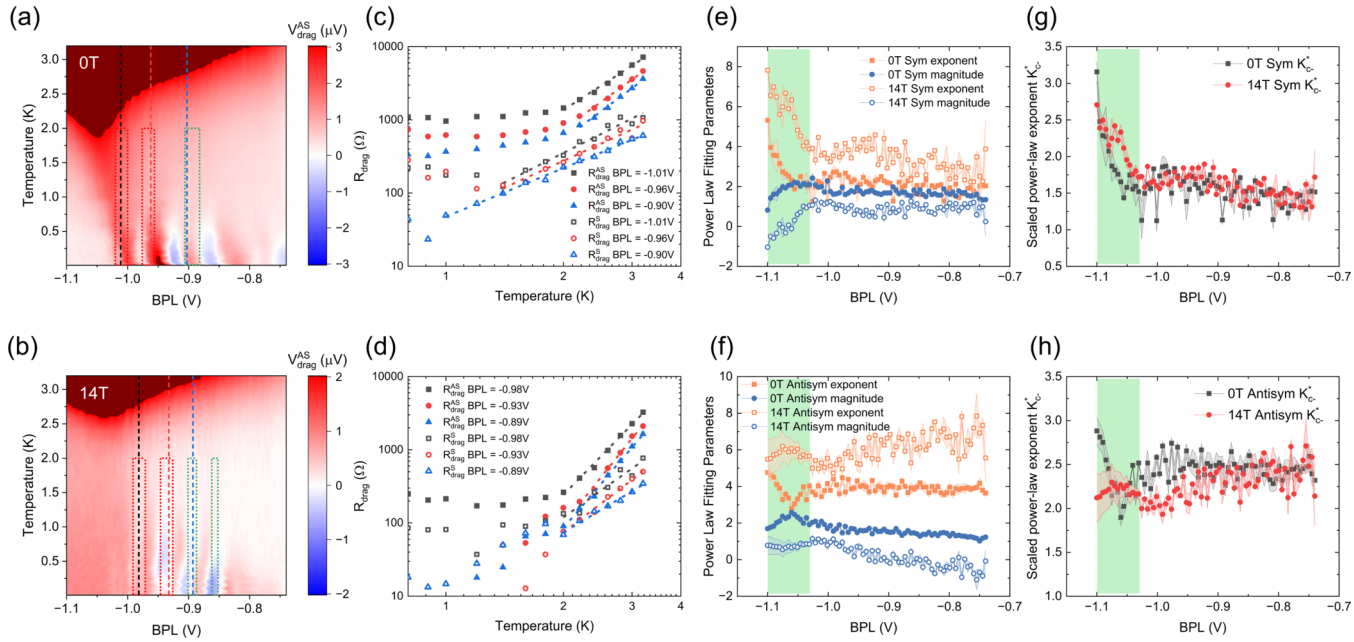

FIG. 2. (a), (b) Antisymmetric component of the Coulomb drag voltage, V_{drag}^{AS}, as a function of BPL gate voltage and temperature at (a) 0 T and (b) 14 T for a line cut at TPL $= -0.424$ V in scan window 1. The red dotted boxes represent the first two defects' positions, while the green dotted boxes represent the first subband at 0 T and the first subband spin-up and spin-down splitting at 14 T. (c), (d) Power-law fitting of three different BPL gate positions, as shown by the dashed lines in panels (a) and (b), respectively. The full symbols represent R_{drag}^{AS}, and the open symbols represent R_{drag}^{S}. The power-law fittings are done in the high-temperature linear range, as shown by the dotted lines. The complete data are shown in Fig. S17 of the Supplemental Material [36]. (e, f) Power-law fitting results of the (e) symmetric component and the (f) antisymmetric component with the 0 and 14 T data shown by the solid symbols and open symbols, respectively. The Arrhenius fitting results are shown in Fig. S16 of the Supplemental Material [36]. (g, h) Extracted K_{c-}^{*} for the two components at 14 and 0 T. The green shaded boxes mark the regions where tunneling is significant, and this regime is not further analyzed in this Letter.

Conductance measurements of the drag wire were performed in magnetic fields ranging from 0 to 14 T. As shown in Figs. 1(c) and 1(d), spin splitting of the first and second subbands is observed with increasing magnetic field at two TPL gate positions, accompanied by a few defect-induced resonances that do not split under the magnetic field. Consistent with previous reports, each spin-degenerate 1D subband N splits into $N\uparrow$ and $N\downarrow$, with the $N\uparrow$ conductance gradually decreasing under increasing magnetic field until it reaches one-half of the original spin-degenerate value [41,42]. Besides, the $N\downarrow$ plateaus vanish around 10 T and reappear at higher fields near 12 T, consistent with prior studies [42] and shown in Fig. 1(c). This transition is attributed to the Zeeman energy $g\mu_B B_{\parallel}$ intersecting the subband energy spacing of around 1.01 meV at 10 T. Corresponding features also appear in the magnetic-field-dependent Coulomb drag signal, as shown in Figs. 1(e) and 1(f). Similar results are observed at different TPL values, as shown in Fig. S13 and in Sec. 5 of the Supplemental Material [36]. Previous works have revealed significant contributions of both reciprocal and nonreciprocal drag signals in similar devices [25], each showing signatures of TLL physics such as an increasing drag signal with decreasing temperature and a power-law temperature dependence of the drag signal combined with an upturn behavior. To investigate these two contributions in the spin-polarized regime, the drag signal is decomposed into a symmetric component, $V_{\mathrm{drag}}^{S} = \frac{V_{\mathrm{drag}}^{R} + V_{\mathrm{drag}}^{L}}{2}$, and an antisymmetric component, $V_{\mathrm{drag}}^{AS} = \frac{V_{\mathrm{drag}}^{R} - V_{\mathrm{drag}}^{L}}{2}$ [25,43]. Here, V_{drag}^{R} is defined as the drag signal for the right-flowing drive current with V_{+} on the left and V_{-} on the right side of the drag wire, and V_{drag}^{L} represents the drag signal for the left-flowing drive current with the drag side unchanged. The magnetic-field dependence of V_{drag}^{AS} is extracted for a line cut at TPL $= -0.402$ V and is shown in Fig. 1(f). V_{drag}^{S} is shown in Fig. S8 of the Supplemental Material [36] and exhibits a similar behavior.

The power-law dependence of the drag signal in the spin-full and spin-polarized regimes is studied by performing temperature-dependent measurements at 0 and 14 T in scan window 1. As shown in Figs. 2(a) and 2(b), V_{drag}^{AS} first decreases with decreasing temperature until a turning temperature $T_0 \sim 1.5$ K, below which it increases as the temperature approaches 0. This nonmonotonic behavior, further discussed in Sec. 4 of the Supplemental Material [36], is consistent with previous observations and is a key signature of TLL physics [23,25–27,33,34]. For $T < T_0$, the drag signal exhibits stripe patterns with alternating signs, which align with conductance plateaus in the drag wire, in agreement with prior results [25]. The temperature dependence of V_{drag}^{AS} and V_{drag}^{S} at selected gate positions is shown in log-log plots with power-law fitting for 0 and 14 T in Figs. 2(c) and 2(d), respectively. Both components can be fitted linearly in the high-temperature regime, indicating power-law behavior, with V_{drag}^{AS} displaying larger magnitudes and steeper slopes than V_{drag}^{S}. In the spin-polarized regime, both components show a reduction in magnitude and

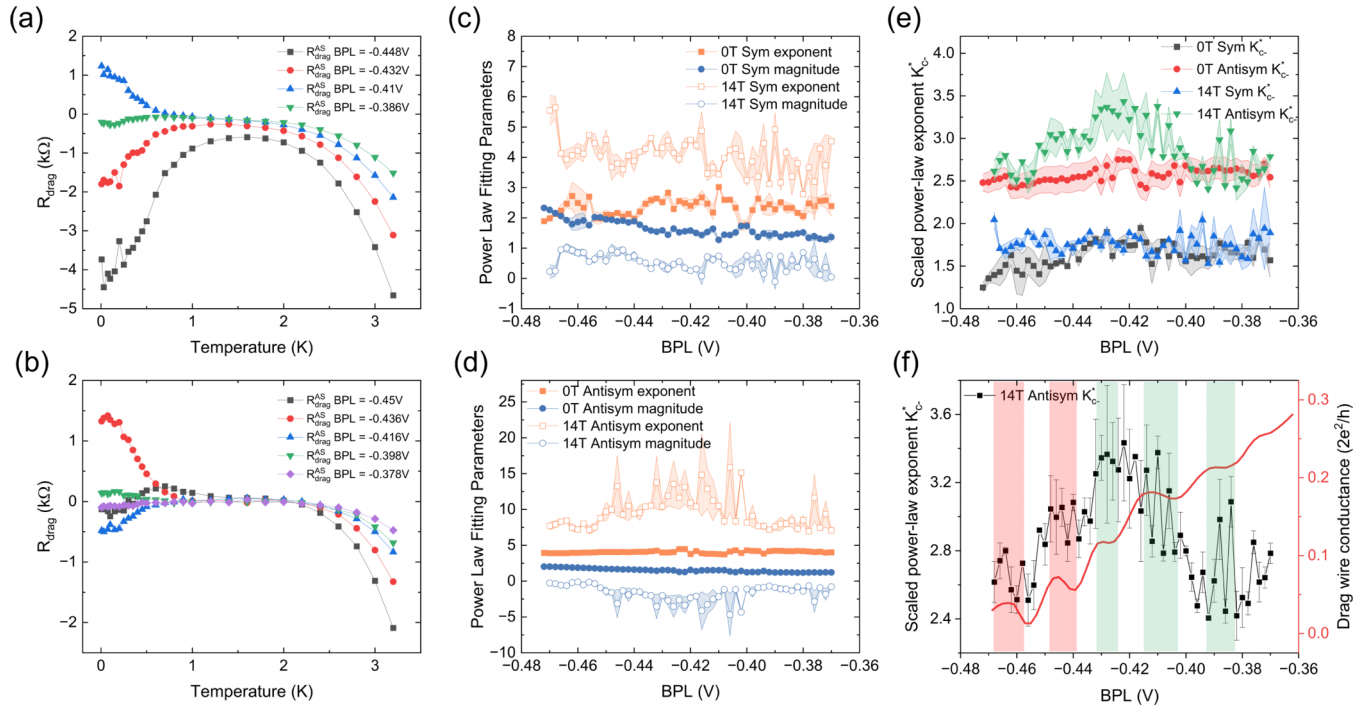

FIG. 3. (a), (b) Temperature dependence of $R^{AS}_{\rm drag}$ at several selected BPL gate positions. $R^{AS}_{\rm drag}$ at 0 T is shown in panel (a) and $R^{AS}_{\rm drag}$ at 14 T is shown in panel (b). (c), (d) Power-law fitting results of the (c) symmetric component and the (d) antisymmetric component at TPL $= -1.095$ V with the 0 and 14 T data shown by the solid symbols and open symbols, respectively. The higher exponents and lower intercepts in 14 T are shown for both symmetric and antisymmetric components. (e) Extracted K^*_{c-} for the two components at 0 and 14 T. (f) Extracted K^*_{c-} for the antisymmetric component at 0 and 14 T and the drag wire conductance at 14 T as a function of the BPL gate positions. The red shades represent the two disorder-induced plateaus, and the green shades represent the first subband spin up plateau, the first subband spin down plateau, and the second subband spin-up plateau from left to right, respectively.

an increase in slope, reflecting a change in the power-law exponents. These effects are more clearly seen by directly comparing the fitting results at 0 and 14 T in Figs. 2(e) and 2(f) for $V^S_{\rm drag}$ and $V^{AS}_{\rm drag}$, respectively. It is worth noting that the signal near the left end of Figs. 2(e) and 2(f) is measured in a regime dominated by tunneling and is not further analyzed in this Letter. In the spin-full regime, the power-law exponents for $V^S_{\rm drag}$ and $V^{AS}_{\rm drag}$ are $x_S \sim 2$ and $x_{AS} \sim 4$, respectively, consistent with previous reports [25]. However, in the spin-polarized regime, the power-law exponents increase to $x_S \sim 3.5$ and $x_{AS} \sim 6$.

While no clear temperature dependence of Coulomb drag in multichannel disordered quantum wires has been predicted, Klesse and Stern [26] have predicted different power-law temperature dependencies for Coulomb drag in the spin-polarized and the spin-full regimes [26] of ballistic quantum wires. At temperatures above that predicted for the formation of two interlocked charge density waves, the Coulomb drag resistance of clean single-channeled quantum wires is predicted to exhibit a power-law temperature dependence, $R_D = R_0\lambda^2(\frac{T}{E_0})^x$, with the power $x = 4K_{c-} - 3$ for spin-polarized wires and $x = 2K_{c-} - 1$ for spin-full wires. Here, R_0 is of order hk_F/e^2, where k_F is the Fermi wave vector; λ denotes the dimensionless interwire backscattering potential; and E_0 is of the order of the Fermi energy. The parameter K_{c-} is the TLL parameter of the relative charge-density sector (antisymmetric density mode). Using the expressions from Klesse and Stern's theory, we extracted the K^*_{c-} of both components at 0 and 14 T, as shown in Figs. 2(g) and 2(h). Throughout this work, we denote the experimentally extracted parameter as K^*_{c-} to distinguish it from the theoretically predicted K_{c-} discussed below, as it is unclear how the extracted power-law in disordered systems relates to the theoretically well-defined K_{c-}. Remarkably, the extracted K^*_{c-} values, around 1.6 and 2.4 for $V^S_{\rm drag}$ and $V^{AS}_{\rm drag}$ respectively, overlap well between the two regimes. This analysis, repeated across three line cuts in scan window 1 and shown in Fig. S14 of Sec. 6 of the Supplemental Material [36], consistently confirms that the K^*_{c-} at 0 and 14 T have similar values. This surprising result extends the power-law scaling prediction for reciprocal drag in clean single-channel wires to the nonreciprocal regime and for multichannel disordered quantum wires.

These results are further confirmed by three line cuts in scan window 2, as shown in Fig. 3 and Fig. S15 of the Supplemental Material [36]. One notable feature is the shift of conductance plateaus toward more negative gate voltages with increasing temperature. This behavior can be attributed to the thermal broadening of the electron distribution or to the effect of the mutual Coulomb interaction [44], and the subband shift has been compensated back to the base temperature in Fig. 3(f). The temperature-dependent $V^{AS}_{\rm drag}$ at a few selected BPL gate positions is shown in Figs. 3(a) and 3(b) for 0 and 14 T, respectively. In addition to the suppression of signal amplitude at higher fields, the turning temperature T_0 increases

from ∼1.6 K at 0 T to ∼2 K at 14 T. The higher T_0 can also be verified through the 2D derivative map $\frac{dV_{\text{drag}}^{AS}}{dT}$, shown in Fig. S8 of the Supplemental Material [36]. We note that the oscillation of K_{c-}^* with gate voltage is further discussed in Sec. 6 of the Supplemental Material [36]. The higher power-law exponents and reduced drag magnitude in the spin-polarized regimes, shown in Figs. 3(c) and 3(d), are consistent with results from scan window 1.

Despite good qualitative agreement with the ballistic 1D drag theory, quantitative details show notable disagreements. Indeed, within the g-ology framework, Klesse and Stern estimate $K_{c-} = \sqrt{\frac{1+U_{c-}}{1-U_{c-}}}$ and $U_{c-} = \frac{1}{2\pi v_{c-}}(-g_2 + \bar{g}_2 + g_1)$, where the forward-scattering terms g_2 and $\bar{g}_2$ and the backscattering term g_1 contribute oppositely to the interaction strength U_{c-} [8,26]. According to these theoretical predictions, the estimated K_{c-} is around 0.994 for spin-full wires and 0.997 for spin-polarized wires using the screening length $D = 142$ nm and the wire width $d = 50$ nm in the single-subband regime of our coupled wires. This estimate does not align with the much larger values of K_{c-}^* reported in this Letter. We point out that the estimate for g_1 was made in the limit of $k_F^{-1} \geqslant d$, which does not apply to our electrically defined quantum wires [26]. In addition, this model was only calculated for the reciprocal drag signal in an ideal system, and our mesoscopic system has both strong reciprocal and nonreciprocal signals, which might account for the mismatch observed here. The discrepancies between K_{c-}^* and the predicted values of K_{c-} stress the importance of further theoretical work considering drag in the nonballistic limit in the presence of electron-electron interactions and nonreciprocal signals. Owing to the limited range of the high-temperature region, we cannot rule out that the drag follows an Arrhenius temperature dependence rather than a power-law. The results from such an analysis are presented in Fig. S16 of the Supplemental Material [36] and yield activation gaps that are independent of gate voltage, which do not match any known theoretical prediction for 1D Coulomb drag.

As previously mentioned, the wires studied in this article host both 1D subbands and disorder arising from the fabrication process. Such disorder could give rise to a nonreciprocal Coulomb drag signal between quantum dots, originating from the nonsymmetrized quantum noise spectrum or the asymmetric coupling to the leads [45,46]. To the best of our knowledge, theory and experiment consistently find that Coulomb drag between quantum dots is either only weakly temperature dependent or strongly suppressed in the low-temperature regime, across a variety of models [22,45–47]. This behavior stands in stark contrast to the pronounced low-T upturn characteristic of 1D systems, a hallmark of Tomonaga-Luttinger liquid physics [26,28,48]. Moreover, quantum-dot-mediated drag is typically significant only near the honeycomb vertices, where the occupancies of both drive and drag dots change, producing a two-dimensional matrix pattern in drag maps rather than the stripelike features we observe (Fig. S6 [36]). In addition, the drive current through quantum dots is expected to be suppressed when the filling is far from a vertex [22,46]. Thus, the observed upturn in temperature dependence, the stripelike drag pattern, and the constant drive current in our 2D maps are strong indications of the predominant 1D origin of the drag signal, although a contribution from coupled quantum dots cannot be entirely ruled out.

In conclusion, we have measured Coulomb drag between closely separated disordered quasi-1D quantum wires in the spin-polarized regime in the presence of both reciprocal and nonreciprocal signals. Consistent with theoretical prediction in clean wires, the same TLL parameter K_{c-}^* extracted from the different power-law exponents of spin-full and spin-polarized wires is reported, both for reciprocal and nonreciprocal drag. Further theoretical work explicitly considering the interplay between disorder, strong electron-electron interactions, and rectification is needed to fully understand the physical origins of $K_{c-}^* > 1$, and its relation to the theoretically predicted K_{c-}; the density dependence of the scattering mechanisms, particularly in multi-subband wires; and the parameter discrepancies between the reciprocal and the nonreciprocal regimes.

This work was supported by the National Science Foundation through Grant No. NSF/DMR-2518016. This work was performed, in part, at the Center for Integrated Nanotechnologies, an Office of Science User Facility operated for the U.S. Department of Energy (DOE) Office of Science. Sandia National Laboratories is a multimission laboratory managed and operated by National Technology & Engineering Solutions of Sandia, LLC, a wholly owned subsidiary of Honeywell International, Inc., for the U.S. DOE's National Nuclear Security Administration under Contract No. DE-NA-0003525. Part of this work was conducted at the Research Service Centers of the Herbert Wertheim College of Engineering at the University of Florida. A portion of this work was also performed at the National High Magnetic Field Laboratory. This work was partially supported by the National High Magnetic Field Laboratory through the NHMFL User Collaboration Grants Program (UCGP). The National High Magnetic Field Laboratory is supported by the National Science Foundation through Grants No. NSF/DMR-1644779 and No. NSF/DMR-2128556 and the State of Florida. A.L. acknowledges financial support by the National Science Foundation under Grant No. DMR-2452658 and by an H. I. Romnes Faculty Fellowship provided by the University of Wisconsin–Madison Office of the Vice Chancellor for Research and Graduate Education with funding from the Wisconsin Alumni Research Foundation.

The views expressed in the article do not necessarily represent the views of the U.S. DOE or the U.S. Government.

Data availability. The data that support the findings of this article are openly available [49].

[1] Y. Cao, V. Fatemi, A. Demir, S. Fang, S. L. Tomarken, J. Y. Luo, J. D. Sanchez-Yamagishi, K. Watanabe, T. Taniguchi, E. Kaxiras, R. C. Ashoori, and P. Jarillo-Herrero, Correlated insulator behavior at half-filling in magic-angle graphene superlattices, Nature (London) **556**, 80 (2018).

[2] V. J. Goldman, M. Santos, M. Shayegan, and J. E. Cunningham, Evidence for two-dimentional quantum wigner crystal, Phys. Rev. Lett. **65**, 2189 (1990).

[3] J. P. Eisenstein and A. H. MacDonald, Bose–Einstein condensation of excitons in bilayer electron systems, Nature (London) **432**, 691 (2004).

[4] Y. Cao, V. Fatemi, S. Fang, K. Watanabe, T. Taniguchi, E. Kaxiras, and P. Jarillo-Herrero, Unconventional superconductivity in magic-angle graphene superlattices, Nature (London) **556**, 43 (2018).

[5] S. Jiang, L. Li, Z. Wang, K. F. Mak, and J. Shan, Controlling magnetism in 2D CrI_3 by electrostatic doping, Nat. Nanotechnol. **13**, 549 (2018).

[6] J. Cai, E. Anderson, C. Wang, X. Zhang, X. Liu, W. Holtzmann, Y. Zhang, F. Fan, T. Taniguchi, K. Watanabe, Y. Ran, T. Cao, L. Fu, D. Xiao, W. Yao, and X. Xu, Signatures of fractional quantum anomalous Hall states in twisted $MoTe_2$, Nature (London) **622**, 63 (2023).

[7] Z. Lu, T. Han, Y. Yao, A. P. Reddy, J. Yang, J. Seo, K. Watanabe, T. Taniguchi, L. Fu, and L. Ju, Fractional quantum anomalous Hall effect in multilayer graphene, Nature (London) **626**, 759 (2024).

[8] J. Voit, One-dimensional Fermi liquids, Rep. Prog. Phys. **58**, 977 (1995).

[9] R. de-Picciotto, M. Reznikov, M. Heiblum, V. Umansky, G. Bunin, and D. Mahalu, Direct observation of a fractional charge, Phys. B (Amsterdam, Neth.) **249-251**, 395 (1998).

[10] A. O. Gogolin, A. A. Nersesyan, and A. M. Tsvelik, *Bosonization and Strongly Correlated Systems* (Cambridge University, Cambridge, England, 2004).

[11] F. D. M. Haldane, Effective harmonic-fluid approach to low-energy properties of one-dimensional quantum fluids, Phys. Rev. Lett. **47**, 1840 (1981).

[12] S. Tomonaga, Remarks on Bloch's method of sound waves applied to many-Fermion problems, Prog. Theor. Phys. **5**, 544 (1950).

[13] J. M. Luttinger, An exactly soluble model of a many-fermion system, J. Math. Phys. **4**, 1154 (1963).

[14] A. G. Rojo, Electron-drag effects in coupled electron systems, J. Phys.: Condens. Matter **11**, R31 (1999).

[15] B. N. Narozhny and A. Levchenko, Coulomb drag, Rev. Mod. Phys. **88**, 025003 (2016).

[16] M. B. Pogrebinskii, Mutual drag of carriers in a semiconductor-insulator-semiconductor system, Sov. Phys. Semicond. **11**, 372 (1977).

[17] T. J. Gramila, J. P. Eisenstein, A. H. MacDonald, L. N. Pfeiffer, and K. W. West, Mutual friction between parallel two-dimensional electron systems, Phys. Rev. Lett. **66**, 1216 (1991).

[18] L. Onsager, Reciprocal relations in irreversible processes. I., Phys. Rev. **37**, 405 (1931).

[19] A. Kamenev and Y. Oreg, Coulomb drag in normal metals and superconductors: Diagrammatic approach, Phys. Rev. B **52**, 7516 (1995).

[20] A. Levchenko and A. Kamenev, Coulomb drag in quantum circuits, Phys. Rev. Lett. **101**, 216806 (2008).

[21] A. Borin, I. Safi, and E. Sukhorukov, Coulomb drag effect induced by the third cumulant of current, Phys. Rev. B **99**, 165404 (2019).

[22] A. J. Keller, J. S. Lim, D. Sánchez, R. López, S. Amasha, J. A. Katine, H. Shtrikman, and D. Goldhaber-Gordon, Cotunneling drag effect in Coulomb-coupled quantum dots, Phys. Rev. Lett. **117**, 066602 (2016).

[23] R. Makaju, H. Kassar, S. M. Daloglu, A. Huynh, D. Laroche, A. Levchenko, and S. J. Addamane, Nonreciprocal Coulomb drag between quantum wires in the quasi-one-dimensional regime, Phys. Rev. B **109**, 085101 (2024).

[24] Y. Fu, Y. Huang, and Q. L. He, Non-reciprocal Coulomb drag between Chern insulators, Nat. Commun. **16**, 3058 (2025).

[25] M. Zheng, R. Makaju, R. Gazizulin, S. J. Addamane, and D. Laroche, Tunable reciprocal and nonreciprocal contributions to 1D Coulomb drag, Nat. Commun. **16**, 6963 (2025).

[26] R. Klesse and A. Stern, Coulomb drag between quantum wires, Phys. Rev. B **62**, 16912 (2000).

[27] M. Pustilnik, E. G. Mishchenko, L. I. Glazman, and A. V. Andreev, Coulomb drag by small momentum transfer between quantum wires, Phys. Rev. Lett. **91**, 126805 (2003).

[28] G. A. Fiete, K. Le Hur, and L. Balents, Coulomb drag between two spin-incoherent Luttinger liquids, Phys. Rev. B **73**, 165104 (2006).

[29] A. P. Dmitriev, I. V. Gornyi, and D. G. Polyakov, Coulomb drag between ballistic quantum wires, Phys. Rev. B **86**, 245402 (2012).

[30] Y. V. Nazarov and D. V. Averin, Current drag in capacitively coupled Luttinger constrictions, Phys. Rev. Lett. **81**, 653 (1998).

[31] M. Bockrath, D. H. Cobden, J. Lu, A. G. Rinzler, R. E. Smalley, L. Balents, and P. L. McEuen, Luttinger-liquid behavior in carbon nanotubes, Nature (London) **397**, 598 (1999).

[32] O. M. Auslaender, H. Steinberg, A. Yacoby, Y. Tserkovnyak, B. I. Halperin, K. W. Baldwin, L. N. Pfeiffer, and K. W. West, Spin-charge separation and localization in one dimension, Science **308**, 88 (2005).

[33] D. Laroche, G. Gervais, M. P. Lilly, and J. L. Reno, Positive and negative Coulomb drag in vertically integrated one-dimensional quantum wires, Nat. Nanotechnol. **6**, 793 (2011).

[34] D. Laroche, G. Gervais, M. P. Lilly, and J. L. Reno, 1D-1D Coulomb drag signature of a Luttinger liquid, Science **343**, 631 (2014).

[35] P. Wang, G. Yu, Y. H. Kwan, Y. Jia, S. Lei, S. Klemenz, F. A. Cevallos, R. Singha, T. Devakul, K. Watanabe, T. Taniguchi, S. L. Sondhi, R. J. Cava, L. M. Schoop, S. A. Parameswaran, and S. Wu, One-dimensional Luttinger liquids in a two-dimensional moiré lattice, Nature (London) **605**, 57 (2022).

[36] See Supplemental Material at http://link.aps.org/supplemental/10.1103/5yqq-cw73 for additional experimental details, data, and analysis.

[37] N. P. R. Hill, J. T. Nicholls, E. H. Linfield, M. Pepper, D. A. Ritchie, A. R. Hamilton, and G. A. C. Jones, Frictional drag between parallel two-dimensional electron gases in a perpendicular magnetic field, J. Phys.: Condens. Matter **8**, L557 (1996).

[38] L. Anderson, A. Cheng, T. Taniguchi, K. Watanabe, and P. Kim, Coulomb drag between a carbon nanotube and monolayer graphene, Phys. Rev. Lett. **127**, 257701 (2021).

[39] L. Du, J. Zheng, Y.-Z. Chou, J. Zhang, X. Wu, G. Sullivan, A. Ikhlassi, and R.-R. Du, Coulomb drag in topological wires separated by an air gap, Nat. Electron. **4**, 573 (2021).

[40] K. Nikolić and A. MacKinnon, Conductance and conductance fluctuations of narrow disordered quantum wires, Phys. Rev. B **50**, 11008 (1994).

[41] K. J. Thomas, J. T. Nicholls, M. Y. Simmons, M. Pepper, D. R. Mace, and D. A. Ritchie, Possible spin polarization

in a one-dimensional electron gas, Phys. Rev. Lett. **77**, 135 (1996).

[42] A. C. Graham, K. J. Thomas, M. Pepper, N. R. Cooper, M. Y. Simmons, and D. A. Ritchie, Interaction effects at crossings of spin-polarized one-dimensional subbands, Phys. Rev. Lett. **91**, 136404 (2003).

[43] M. Zheng, R. Makaju, R. Gazizulin, A. Levchenko, S. J. Addamane, and D. Laroche, Quasi-1D Coulomb drag in the nonlinear regime, Phys. Rev. Lett. **134**, 236301 (2025).

[44] S. Tarucha, T. Honda, and T. Saku, Reduction of quantized conductance at low temperatures observed in 2 to 10 μm-long quantum wires, Solid State Commun. **94**, 413 (1995).

[45] K. Kaasbjerg and A.-P. Jauho, Correlated Coulomb drag in capacitively coupled quantum-dot structures, Phys. Rev. Lett. **116**, 196801 (2016).

[46] M. A. Sierra, D. Sánchez, A.-P. Jauho, and K. Kaasbjerg, Fluctuation-driven Coulomb drag in interacting quantum dot systems, Phys. Rev. B **100**, 081404(R) (2019).

[47] R. Sánchez, R. López, D. Sánchez, and M. Büttiker, Mesoscopic Coulomb drag, broken detailed balance, and fluctuation relations, Phys. Rev. Lett. **104**, 076801 (2010).

[48] T. Fuchs, R. Klesse, and A. Stern, Coulomb drag between quantum wires with different electron densities, Phys. Rev. B **71**, 045321 (2005).

[49] M. Zheng, R. Makaju, R. Gazizulin, A. Levchenko, S. Addamane, and D. Laroche, Repository for Quasi-1D Coulomb drag between spin-polarized quantum wires, Zenodo (2026), doi:10.5281/zenodo.18744775.